

The Renaissance of Poly(3-hexylthiophene) as a Promising Hole-Transporting Material Toward Efficient and Stable Perovskite Solar Cells

Xiaozhen Huang, Xuran Wang, Yaqing Zou, Mingwei An,* and Yang Wang*

To push the commercialization of the promising photovoltaic technique of perovskite solar cells (PSCs), the three-element golden law of efficiency, stability, and cost should be followed. As the key component of PSCs, hole-transporting materials (HTMs) involving widely-used organic semiconductors such as 2,2',7,7'-tetrakis-(*N,N*-di-4-methoxyphenylamino)-9,9'-spirobifluorene (Spiro-OMeTAD) or poly(triarylamine) (PTAA) usually suffer high-cost preparation and low operational stability. Fortunately, the studies on the classical p-type polymer poly(3-hexylthiophene) (P3HT) as an alternative HTM have recently sparked a broad interest due to its low-cost synthesis, excellent batch-to-batch purity, superior hole conductivity as well as controllable and stable film morphology. Despite this, the device efficiency still lags behind P3HT-based PSCs mainly owing to the mismatched energy level and poor interfacial contact between P3HT and the perovskite layer. Hence, in this review, the study timely summarizes the developed strategies for overcoming the corresponding issues such as interface engineering, morphology regulation, and formation of composite HTMs from which some critical clues can be extracted to provide guidance for further boosting the efficiency and stability of P3HT-based devices. Finally, in the outlook, the future research directions either from the viewpoint of material design or device engineering are outlined.

of clean and renewable solar energy. Over the past few decades, crystalline silicon (C-Si) solar cells and thin-film cadmium telluride (CdTe) or copper indium gallium selenide sulfide (CIGS) solar cells have emerged as the first and second-generation photovoltaic technology, respectively.^[1,2] However, they suffer from high production costs, high environmental pollution, and long payback time although they still dominate the commercial photovoltaic market nowadays. Encouragingly, the advent of solution-processable solar cells (e.g., dye-sensitized solar cells,^[3] organic solar cells,^[4] quantum dot solar cells^[5] and perovskite solar cells^[6]) at the end of last century may blow fresh air into the photovoltaic field due to their shortened production line and low-cost manufacturing, among which perovskite solar cells (PSCs) hold the greatest promise for the next-generation photovoltaic applications owing to their significantly high power conversion efficiency (PCE) and flexibility in integrating with other photovoltaic cells.^[7–10]

Generally, PSCs incorporate organic-inorganic lead halide perovskite materials

as the key light absorber, along with a hole-transporting layer, electron-transporting layer, and electrodes, forming a sandwiched-like device structure. Depending on different deposition sequences, PSCs are usually divided into two types, i.e., conventional (n-i-p) and inverted (p-i-n) architectures. Up to date, the state-of-the-art PSCs showing PCE exceeding 25% are mostly based on n-i-p structures, including the record-breaking device with 26.1% certified efficiency.^[11] It is noteworthy that most of the top-performing n-i-p PSCs rely on the organic small molecular hole-transporting material (HTM) 2,2',7,7'-tetrakis(*N,N*-di-4-methoxyphenylamino)-9,9'-spirobifluorene (Spiro-OMeTAD)^[12] or polymeric HTM poly(triarylamine) (PTAA)^[13] due to their stable amorphous film morphologies, well-matched energy levels and good universality in different optoelectronic devices. Nevertheless, to achieve high efficiency, it is unavoidable to introduce p-type dopants to enhance the hole conductivity of such HTMs which would conversely sacrifice the device stability. In this regard, exploration of novel dopant-free HTMs has become research hotspot in recent years, including small molecules,^[14] polymers,^[15] dendrimers,^[16] and composite HTMs.^[17] Despite

1. Introduction

To alleviate the global fossil energy crisis, photovoltaic technology which can directly convert light sources into electric energy is regarded as the most important solution due to the effective harvest

X. Huang, X. Wang, Y. Zou, M. An, Y. Wang
Strait Institute of Flexible Electronics (SIFE
Future Technologies)
Fujian Key Laboratory of Flexible Electronics
Fujian Normal University and Strait Laboratory of Flexible Electronics
(SLoFE)
Fuzhou, Fujian 350117, China
E-mail: ifemwan@fjnu.edu.cn; ifewangy@fjnu.edu.cn
Y. Wang
State Key Laboratory of Structural Chemistry
Fujian Institute of Research on the Structure of Matter
Chinese Academy of Sciences
Fuzhou, Fujian 350002, China

The ORCID identification number(s) for the author(s) of this article can be found under <https://doi.org/10.1002/sml.202400874>

DOI: 10.1002/sml.202400874

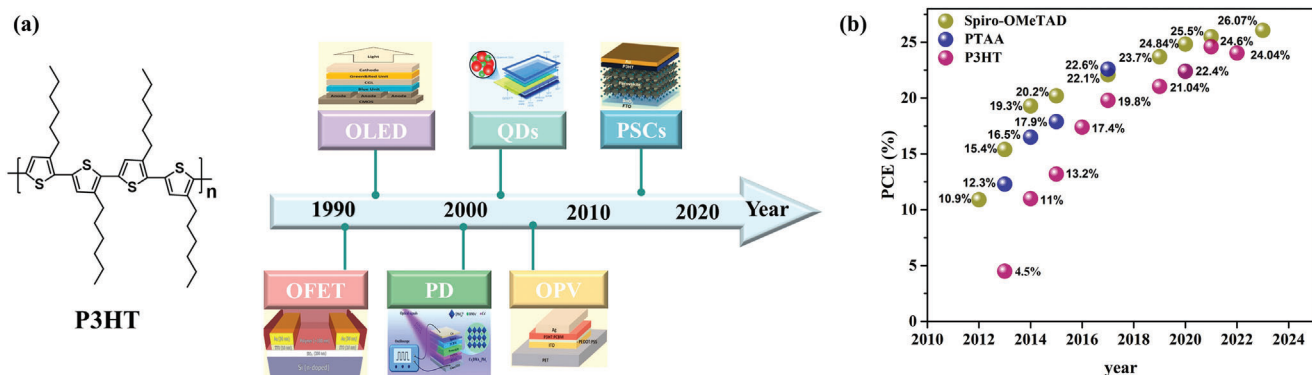


Figure 1. a) The development trend of P3HT applied in different optoelectronic devices. b) The progress of PSCs incorporating Spiro-OMeTAD, PTAA, and P3HT as HTMs, respectively.

this, the device performance based on dopant-free HTMs is still lagging behind Spiro-OMeTAD-based devices. Moreover, some dopant-free HTMs suffer tedious synthetic procedures, difficult purification, poor batch-to-batch variation, and low reproducibility in different research groups. Therefore, considering the three vital figure-of-merits (efficiency, cost, stability) for the commercialization of PSCs, the design criteria of promising HTMs should be low-cost, dopant-free, along with high chemical stability and universality.^[18]

In retrospect, the most original is often the best. The classical polymeric organic semiconductor, regioregular poly(3-hexylthiophene) (P3HT) which was developed in the early 1990s, has been the predominant p-type conjugated polymer and a mainstay of research in various organic optoelectronic devices, such as organic field-effect transistors (OFETs),^[19] organic solar cells (OSCs),^[20] quantum dot solar cells (QSCs),^[21] organic light-emitting diodes (OLEDs),^[22] and photodetectors (PDs)^[23] (Figure 1a). The superior application universality of P3HT is ascribed to its easy and inexpensive preparation, fine-tuned morphology, excellent charge mobility, high chemical stability, and high tensile modulus.^[24,25] So come back to the newfangled PSCs, P3HT is also expected to be a promising HTM to realize efficient and stable devices. Actually, since the first report of P3HT acting as HTM in n-i-p PSCs,^[26] numerous research efforts have been rekindled to further explore the potential of P3HT in efficient and highly stable PSCs. It is known that when utilized in PSCs, the mismatched energy level with the valence band (VB) of perovskite and poor interfacial contact between P3HT and perovskite are the two main obstacles that limit the device's performance. Fortunately, by specific modulation of P3HT morphology and/or interface engineering, the P3HT-based PSCs achieved significant progress during the past years with the highest PCE exceeding 24%.^[27] Importantly, the device stability was remarkably enhanced compared to the PSCs based on doped HTM systems.

As there is still much room for the improvement of P3HT-based PSCs, in this review, we aim to fully summarize the development of PSCs based on P3HT HTM. Specifically, a brief description of P3HT was first presented including the discovery, synthesis, and basic properties of P3HT. Then the requirements for the design of suitable HTMs in n-i-p PSCs were put forward along with the comparison of several widely used

HTMs. Next, focused on P3HT, various strategies aiming to tune energy level and energetics, improve hole conductivity, regulate film morphology as well as optimize interfacial contact were summarized from which some critical clues could be extracted to provide guidance for further boosting the efficiency and stability of P3HT-based devices. Finally, we provide insights and prospects on the future research direction with respect to developing more efficient strategies to further enhance the performance of P3HT-based PSCs probably by the combination of molecular design, interface treatment, and device engineering.

2. P3HT: A Brief Retrospect

Since the discovery of organic conductive polymers in the 1970s,^[28] more attention has been paid to the exploration of organic semiconducting materials with specific optoelectronic properties. Thereinto, thiophene is a well-known simple conjugated monomer with an electron-rich aromatic ring that can be polymerized to form long conjugated chains and show decent hole transport ability. However, to facilitate the solubility of polythiophenes (PTs), the alkyl chain should be introduced to the 3-position of thiophene ring which may lead to regiorandom PTs because the coupling reaction of 3-substituted thiophene at the 2- and 5-positions is usually uncontrollable and different regioisomeric triads in the polymer chain are prone to form. Fortunately, a breakthrough was made by Rieke and McCullough in the synthesis of highly regioregular P3HT in the 1990s which involved a Kumada-like polycondensation.^[29,30] This polymerization features a quasi-living mechanism and is also called the Grignard metathesis method which needs a nickel(II) catalyst to reinforce the regioselectivity of the Grignard exchange.^[31] As a consequence, the regioregularities of head-to-tail couplings in the polymer chain can be obtained above 98%, and the degrees of polymerization can be very high (>100) along with a narrow distribution of molecular weights (MWs) (dispersity <1.5).

The degree of regioregularity has a significant effect on the properties of P3HT such as electronic and morphological properties. It was found that the dominant head-to-tail arrangement of thiophene monomers facilitates coplanarity of polymer backbone in regioregular P3HT which enables efficient packing and

better intra- and intermolecular overlap, whereas the regionandom P3HT has a twisted conformation, which usually suffers limited conjugation length, poor intermolecular packing, and low crystallinity.^[25] Benefited from ordered molecular structure, highly regioregular P3HT can achieve high crystallinity in the solid state, high hole mobility ($\mu_h > 0.1 \text{ cm}^2 \text{ V}^{-1} \text{ s}^{-1}$) in the pristine film and smaller bandgap of $\approx 1.9\text{--}2.0 \text{ eV}$ which are beneficial for applications in organic optoelectronic devices.^[32] Furthermore, since the backbone of P3HT is made only of isolated thiophene rings and linear hexyl chains, the polymer chains have significant freedom to assemble specific packing motifs and consequently, the morphological properties can be finely tuned depending on the technique of deposition. The glass transition temperature (T_g) of P3HT is less than room temperature ($\approx 13^\circ \text{C}$) and the melting point is above 200°C .^[33] The polymers with low T_g are good candidates for stretchable semiconducting thermoplastics which may show good adhesion and mechanical durability during the solution process. Also, P3HT features a high tensile modulus^[34] by the standards of soft materials: 200 MPa to 1 GPa depending on the temperature, sample purity, and testing method. Due to the cheap raw materials and simple chemical structure as well as the mature synthetic process, the cost of P3HT is sharply lowered for large-scale preparation in the current stage and the MW can be well controlled along with low polydispersity. Therefore, the promising merits of low cost, high chemical stability, superior hole mobility, and controllable film morphology endow P3HT with high potential in the application of organic semiconductor devices.

3. P3HT as HTM in PSCs

As a key component in PSCs, HTM plays a critical role in extracting holes and blocking electrons at the interface between perovskite and HTM, transporting holes to anode as well as optimizing interfacial contact so as to reduce nonradiative recombination and improve interface stability. Hence, several criteria should be required to meet the demand for designing efficient HTMs:^[35] i) appropriate energy-level alignment, i.e., the highest occupied molecular orbital (HOMO) of HTMs should be slightly shallower than the VB of perovskite to facilitate hole extraction and minimize the energy losses at interfaces, meanwhile, the lowest unoccupied molecular orbital (LUMO) of HTMs should be high enough to block electrons to suppress the charge recombination; ii) high hole mobility and conductivity to enable efficient hole transport from perovskite to electrode; iii) high stability including chemical, thermal and operational stability; iv) superior film quality with high uniformity, appropriate wetting property as well as additional functions such as passivation effect and barrier to inhibit oxygen/water permeation; v) low-cost preparation and eco-friendly processability. To achieve these properties, a wide range of HTMs from inorganic compounds to organic small molecules and polymers has been explored over the past decade.^[36–38] However, the most popular and universal HTM remains Spiro-OMeTAD, which was initially synthesized in the 1990's^[39] and first applied in PSCs in 2012 demonstrating an impressive efficiency of 9.7%.^[40] The enduring popularity and good universality of Spiro-OMeTAD as an HTM in PSCs

can be ascribed to its straightforward synthesis, excellent solubility in various common solvents, ease of processing, and amorphous and stable film morphology. Moreover, the doping strategy can lower down its HOMO level to well match the VB of perovskite and simultaneously enhance its hole conductivity.^[41] To date, the PCE of Spiro-OMeTAD-based PSCs has surpassed 26% which can play against crystalline silicon photovoltaics^[42,43] (Figure 1b). However, just because of the introduction of dopants, the T_g of Spiro-OMeTAD film is dramatically lowered to below 80°C which may apparently compromise the thermal stability of the device. Even worse, the dopants may move and aggregate during long-time operation due to their rather small structures so that phase separation and ion migration may occur which will induce unstable film morphology and interface degradation.^[44] In a word, the PSCs incorporating doped Spiro-OMeTAD inevitably suffer severe operational instability especially under harsh conditions (ISOS-D3)^[45] which is a significant roadblock to further commercial applications. As another widely-used HTM, PTAA was initially employed as an HTM in PSCs in 2013, demonstrating a PCE of up to 12%. The incorporation of dopants such as lithium bis(trifluoromethanesulfonyl)imide (Li-TFSI) and 4-tert-butylpyridine (tBP) enables higher device performance of PTAA-based PSCs than that of Spiro-OMeTAD.^[46] PTAA exhibits a heightened affinity for perovskite at the interface, potentially leading to an increased extraction of holes. Also, PTAA features stable amorphous film with high thermal stability. The ongoing research has boosted the PCE of PTAA-based PSCs beyond 22%^[47] (Figure 1b). Nevertheless, PTAA suffers from high-cost preparation, poor batch-to-batch quality, and especially low intrinsic hole mobility which unavoidably need additional dopants to enhance its electronic properties as the same for Spiro-OMeTAD.^[48] The incorporation of dopants may lead to a decreased lifetime of devices. In this context, exploring novel low-cost and stable functional HTMs without the usage of dopants is an urgent need. By adopting various chemical design strategies, an ample variety of dopant-free HTMs have been developed in recent years which, however, still lack top-notch device performance and good universality.^[49–52] As such, the widely-studied p-type semiconductor P3HT has revived the interest of researchers due to its unique properties and commercialized production which is easier for the joint research of different groups. P3HT can be obtained in bulk quantities with low-cost synthesis and excellent batch-to-batch quality. In addition, P3HT features an ordered molecular structure and can achieve high crystallinity in the solid state which enables high hole mobility in the pristine film as stated in Section 2. Such superior electronic properties of P3HT can avoid the usage of dopants and enable good performance in dopant-free devices. Until now, the PSCs involving P3HT as HTM have realized a remarkably high PCE of 24.6% with superior stability which can maintain 99% of the initial PCE for 2000 h under 85% relative humidity at room temperature without encapsulation.^[27,53] In this section, we will first introduce the universal application of P3HT as HTM in different types of PSCs, then more attention will be focused on the developed strategies for enhancing the device performance of P3HT-based PSCs such as interface engineering, morphology regulation, formation of composite HTMs, and derived modification of P3HT and its future applications.

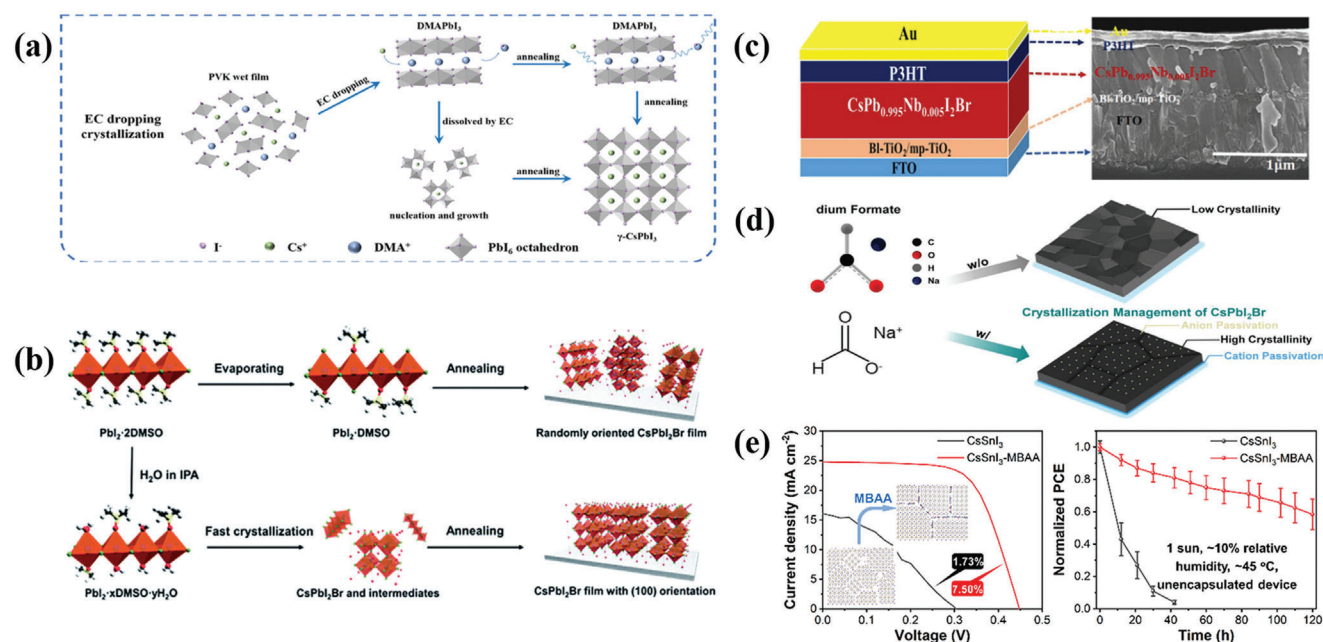


Figure 2. a) Schematic diagram of the EC dropping crystallization progress. Reproduced with permission. Copyright 2023, John Wiley and Sons.^[61] b) Plausible formation mechanisms of CsPbI₂Br perovskite film. Reproduced with permission.^[62] Copyright 2020, Royal Society of Chemistry. c) Schematic representation of the device configuration and cross-sectional SEM image of the Nb-CsPbI₂Br-based device. Reproduced with permission.^[63] Copyright 2020, American Chemical Society. d) A schematic illustration of the sodium formate (NaFo) effect on inorganic CsPbI₂Br perovskite film. Reproduced with permission.^[64] Copyright 2023, John Wiley and Sons. e) Schematic illustration of the MBAA treating the CsSnI₃-based device and operational stability assessment without encapsulation. Reproduced with permission.^[65] Copyright 2021, American Chemical Society.

3.1. General Application of P3HT in PSCs

Since the PSCs incorporating P3HT as HTM debuted in 2013 with a fair efficiency of 4.5%,^[26] considerable efforts have been evoked to follow the investigation of P3HT-based PSCs. By optimizing the thickness of MAPbI₃ perovskite layer, Liu et al. reported an 11.3% PSC based on P3HT using the vapor-phase deposition method of the Pbl₂ precursor film.^[54] Later, they revealed an electron-transporting layer (ETL)-a free device with an efficiency of 11.6% using undoped P3HT.^[55] In 2017, Colodrero et al. boosted the efficiency of MAPbI₃-based PSCs to 14.4% using P3HT which shows better performance than that involving a donor-acceptor polymer as HTM.^[56] Recently, Chauhan et al. showed that the deposition temperature of MAPbI₃ film may significantly affect the micro/ nanostructures on the perovskite surface as well as the resultant interface between perovskite/P3HT.^[57] When changing the perovskite composition from MAPbI₃ to MAPbI_{3-x}Br_x^[58] and MAPbI_{3-x}Cl_x,^[59] the PSCs based on pristine P3HT could achieve moderate PCEs of 6.64% and 13.6%, respectively. Yang et al. developed an intelligent spin-joint decomposition strategy to create in situ P3HT/perovskite heterogeneous interfaces featuring an interpenetrating network structure. This approach aims to reduce defects and enhance energy alignment at the PVK/HTL interface which can address the issue of inadequate physical contact between P3HT and perovskite. As a result, the remarkably high PCE of 24.53% could be realized.^[60] Moreover, even for all-inorganic PSCs, P3HT could still show attractive efficiency as a dopant-free HTM. For example, Ren et al. incorporated P3HT as a dopant-free HTM to CsPbI₃-based PSCs where ethyl cyanoformate (EC) was adopted

as an antisolvent to reduce the annealing temperature and enable high-quality perovskite film. As a result, a high PCE of 18.46% was achieved along with excellent operational stability (90% of initial PCE was maintained over 170 h) (Figure 2a).^[61] Lin et al. reported an appealing PCE of 16.74% for P3HT-coated CsPbI₂Br PSCs which involves water and isopropanol to assist the formation of highly oriented perovskite film (Figure 2b).^[62] Moreover, by utilizing dopants or additives in the perovskite solutions (such as Nb ion^[63] or sodium formate),^[64] the enlarged grain size and reduced trap density could be realized for CsPbI₂Br film, and consequently enhanced PCEs of 16.45% and 17.7% could be obtained, respectively, along with higher air and phase stability (Figure 2c,d). To mitigate the toxicity of lead-based perovskite materials, tin (Sn) based PSCs have begun to attract a great deal of attention in recent years. However, the easier oxidation of Sn²⁺ in Sn-based perovskites is conceived as the biggest issue influencing the device's performance and stability. Priya et al. utilized N,N'-methylenebis(acrylamide) to form coordination bonding with Sn²⁺ and reduce defect (Sn⁴⁺) density which can stabilize the black orthorhombic (B-γ) phase of CsSnI₃. By depositing P3HT on CsSnI₃ perovskite, an attractive PCE of 7.5% was documented with high ambient-air stability (Figure 2e).^[65]

3.2. Interface Engineering for P3HT-Based PSCs

As reviewed in the above section, P3HT exhibits good universality when applied in PSCs with various perovskite active layers due to its suitable optoelectronic properties and stable morphological properties. However, the mismatched

Table 1. Interfacial engineering in P3HT-based PSCs.

Perovskite composition	Interfacial engineering	PCE (%)	Stability assessment	Refs.
CsPbI ₂ Br	(poly[(9,9dioctylfluorenyl-2,7-diyl)-co-(4,4'-(N-(4-sec-butylphenyl)diphenylamine)) (TFB)	15.50	SS: over 95% PCE retained (1500 h, below 25% RH, ambient)	[66]
(Cs _{0.05} FA _{0.54} MA _{0.41}) Pb(I _{0.98} Br _{0.02}) ₃	butylamine modified poly[3-(4-carboxylatebutyl) thiophene] (P3CT-BN)	19.23	SS: 80% PCE retained (2300 h, 50% RH, 25 °C) TS: 80% PCE retained (400 h, N ₂ , 85 °C) as well as 79% PCE retained (386 h, 60–70% RH, 60 °C) OS: 96% PCE retained (34 h, MPP)	[67]
CsPbI ₂ Br	thienylmethylamine acetate (ThMAAc) + BTCIC-4Cl	16.3	TS: 97% PCE retained (530 h, N ₂ , 85 °C) without any encapsulation	[68]
FAPbI ₃	1-hexyl-2,5-dimethyl-1H-pyrrole-3-carboxylic acid (HPCA)	20.78	SS: over 80% PCE retained (1000 h, ≈60 RH, 25 °C) without encapsulation. TS: over 80% PCE retained (530 h, N ₂ , 85 °C). OS: over 80% PCE retained (400 h, continuous illumination, ambient)	[69]
FA _{0.90} Cs _{0.07} MA _{0.03} PbI _{2.76} Br _{0.24}	3,3'-(2,7-bis(3,6-bis(bis(4-methoxyphenyl)amino)-9H-carbazol-9-yl)9H-fluorene-9,9-diyl)bis(N,N,N-trimethylpropan-1-aminium) iodide (MPA-Cz-PAI)	19.7	SS: over 85% PCE retained (1500 h, 70% RH, ambient) without encapsulation	[70]
(FAPbI ₃) _{0.95} (MAPbBr ₃) _{0.05}	octylammonium azide (OAN ₃)	20	SS: 90% and 80% retained (with cross-linking and without cross-linking) of initial PCE after 500 h under 50–60% RH at ambient without any encapsulation.	[71]
MAPbI ₃	perovskite quantum dots (CsPbI _{1.85} Br _{1.15})	21.1	OS: PCE nearly keeping unchanged (10 000 h, 65% RH, 25 °C) with encapsulation	[73]
(FAPbI ₃) _{0.95} (MAPbBr ₃) _{0.05}	ultrathin wide-bandgap halide (MAPbBr ₃)	23.3	SS: 80% PCE retained (1008 h, 85% RH, RT) without encapsulation. OS: 95% PCE retained (1370 h, continuous illumination, RT) with encapsulation	[74]

SS: Storage Stability; **OS:** Operational Stability; **TS:** Thermal Stability.

energy level, strong electronic coupling, poor physical contact, and undesirable nonradiative recombination losses at the perovskite/P3HT interface severely limit the device's efficiency. To overcome these issues, various strategies have been developed such as designing new functional materials, polishing interface contact, controlling morphology, and optimizing device structure, which will be thoroughly reviewed starting in this section (Tables 1 and 2).

To reduce the carrier recombination at the interface of perovskite and P3HT, Hu et al. introduced a polymer (poly[(9,9dioctylfluorenyl-2,7-diyl)-co-(4,4'-(N-(4-sec-butylphenyl)diphenylamine)) (TFB as acronyms) as a buffer layer to improve the energy level alignment between CsPbI₂Br perovskite and P3HT. The implementation of TFB significantly enhances the separation and extraction of carriers at the interfaces, hence, a high open-voltage (V_{oc}) of 1.26 V was realized accompanied by the champion PCE of 15.5%. Also, the P3HT-treated device shows much enhanced ambient stability with over 95% PCE after 1300 h as opposed to Spiro-OMeTAD (Figure 3a).^[66] By incorporating a polyelectrolyte buffer layer, i.e., butylamine modified (poly[3-(4-carboxylatebutyl) thiophene] (P3CT-BN), Zhang et al. found that the P3HT film morphology, perovskite built-in electric field, surficial defects, and the hole

transfer efficiency were all optimized as well as the reduced interfacial recombination. Consequently, a high PCE of 19.23% could be achieved along with excellent stability for unencapsulated devices which retain 79% of the original PCE under simultaneous damp heat (60 °C/60–70% humidity) in the air for 386 h.^[67]

Later, Bi et al. demonstrated a multi-strategy to improve P3HT-based all-inorganic PSCs with thienylmethylamine acetate as an additive in the precursor solution of perovskite to enhance the α phase stability and passivate the bulk defects and small molecule namely BTCIC-4Cl as interlayer at the CsPbI₂Br/P3HT interface to suppress surface defects. It was shown that the robust interaction between BTCIC-4Cl and thiophene units within P3HT could improve the extraction of charge carriers and promote hole transport. The resultant device achieved the highest PCE of 16.3% and retained 97% of original efficiency after aging for 500 h at 85 °C.^[68] To optimize interfacial properties, Gu et al. designed and synthesized a multifunctional molecule 1-hexyl-2,5-dimethyl-1H-pyrrole-3-carboxylic acid (HPCA) whose carboxyl group could effectively passivate the undercoordinated Pb²⁺ defects and hexyl substituted pyrrole could improve the physical contact and favor self-assembly of P3HT on the perovskite film, thus the electron overlapping and delocalization between the

Table 2. Formation of composite HTMs in P3HT-based PSCs.

Perovskite composition	Composite HTMs	PCE (%)	Stability assessment	Refs.
MAPbI _{3-x} Cl _x	single-walled carbon nanotubes (SWNTs)/P3HT	15.3	SS: PCE retained unchanging after water exposure for 60 s	[95]
MAPbI ₃	Graphdiyne (GD)/P3HT	14.58	SS: over 90% PCE retained (15 weeks, dry environment, RT) without encapsulation	[96]
CH ₃ NH ₃ PbI ₃	4% functional-graphene/P3HT	13.82	SS: 70% PCE retained (8 weeks, 20–40% RH, RT)	[97]
CsPbI ₂ Br	SMe-TATPyr/P3HT	16.93	SS: 96% PCE retained (1500 h, 10–20% RH, air ambient) without encapsulation. TS: 95% PCE retained (1000 h, 85 °C, N ₂)	[98]
Cs _{0.05} FA _{0.85} MA _{0.10} Pb(Br _{0.03} I _{0.97}) ₃	2-((7-(4-(bis(4-methoxyphenyl)amino)phenyl)-10-(2-(2-ethoxyethoxy)ethyl)-10H-phenoxazin-3yl)methylene)malononitrile (MDN)/P3HT	22.87	SS: ≈92% PCE retained (30-day, 85% RH, 25 °C) without encapsulation	[99]
(FA _{0.83} MA _{0.17}) _{0.95} Cs _{0.05} Pb(I _{0.9} Br _{0.1}) ₃	NiO _x /P3HT	21.2	OS: 80% PCE retained (10 000 min, AM 1.5 G, 50% RH, 85 °C) with encapsulation. TS: 91% PCE retained (1000 h, 85% RH, 85 °C) with encapsulation	[100]
Cs _{0.05} (MA _{0.13} FA _{0.87}) _{0.95} Pb(I _{0.87} Br _{0.13}) ₃	gold nanorod (AuNR)/P3HT	16.88	SS: over 60% PCE retained (400 h, 75% RH, room light, 25 °C) without encapsulation	[101]
CsPbBr ₃	zinc phthalocyanine (ZnPc)/P3HT	10.03	SS: 98% PCE retained (30 days, 70% RH, 20 °C) without encapsulation	[102]
Cs _{0.05} FA _{0.88} MA _{0.07} PbI _{2.56} Br _{0.44}	copper phthalocyanine (CuPc)/P3HT	23.17	OS: ≈95.3% PCE retained (260 h, 85% RH, 85 °C) with encapsulation. TS: ≈91.7% PCE retained (1009 h, 85% RH, 85 °C) with encapsulation	[103]
(FAPbI ₃) _{0.95} (MAPbBr ₃) _{0.05}	gallium(III) acetylacetonate (GA(acac) ₃)/P3HT	24.6	SS: 99% PCE retained (2000 h, 85% RH, RT) without encapsulation. TS: over 80% PCE retained (408 h, 10% RH, 85 °C) without encapsulation	[27]

SS: Storage Stability; **OS:** Operational Stability; **TS:** Thermal Stability.

pyrrole unit in HPCA and the thiophen unit in P3HT could be reinforced to facilitate hole extraction and transport. As a consequence, the HPCA-treated FAPbI₃-based PSC using P3HT as HTM could achieve a remarkably high PCE of 20.78% along with superior storage stability (80% of initial PCE after 1000 h under 65% relative humidity (RH)) and thermal stability (80% of original PCE after 500 h at 80 °C) (Figure 3b).^[69] Different from traditional organic molecules, ionic molecules with intrinsic ion pairs are also regarded as good candidates for interface passivators due to their controllable hydrophobicity or hydrophilicity and the tendency to form build-in internal electric field. Wang et al. designed and synthesized ionic dendrimers with quaternary ammonium iodide as the side chains. The dendritic backbone built up with carbazole and diphenylamine units ensures high thermal stability, well-matched energy level, and good hole mobility, while the ionic side chains enable good solubility, appropriate hydrophobicity, and enhanced interfacial compatibility. It was also found that such ionic dendrimers can not only enhance the conductivity of the P3HT by regulating the microstructure of polymers but also inhibit the surface defects of perovskite. As a result, by using the ionic dendrimers as an interlayer between perovskite and P3HT, a high PCE approaching 20% was achieved accompanied by excellent storage stability under high humidity conditions

(Figure 3c).^[70] Choi et al. adopted an ionic molecule octylammonium azide (OAN₃) as the interfacial layer. Apart from the passivation effect enabled by ammonium ions, the azide group acting as a cross-linking site with P3HT can reinforce the interfacial contact between perovskite and P3HT. Consequently, the device with OAN₃-treated PSCs could achieve a considerably high PCE of 20.0% (Figure 3d). Importantly, the PSCs treated with OAN₃ are able to retain 90% and 82% of the original efficiency under 50–60% RH conditions (with or without cross-linking). However, the PCE of PSCs lacking OAN₃ sharply decays to only 38% of the initial value under the same conditions.^[71]

Besides organic molecules, perovskite quantum dots (QDs) can be applied as buffer layers to modulate the interface of perovskite and P3HT due to their adjustable energy bands and high chemical compatibility with common HTMs.^[72] Wu et al. investigated the multifunction of QD interlayers between P3HT and perovskite and found that they can not only passivate the perovskite surface to reduce the overall amount of trap states and promote hole extraction by forming cascade energy levels but also regulate the orientation of P3HT and improve hole mobility. Encouragingly, a maximum PCE of 21.1% was realized outperforming that based on pristine P3HT (16.0%) along with improved device stability (Figure 3e).^[73] A breakthrough in

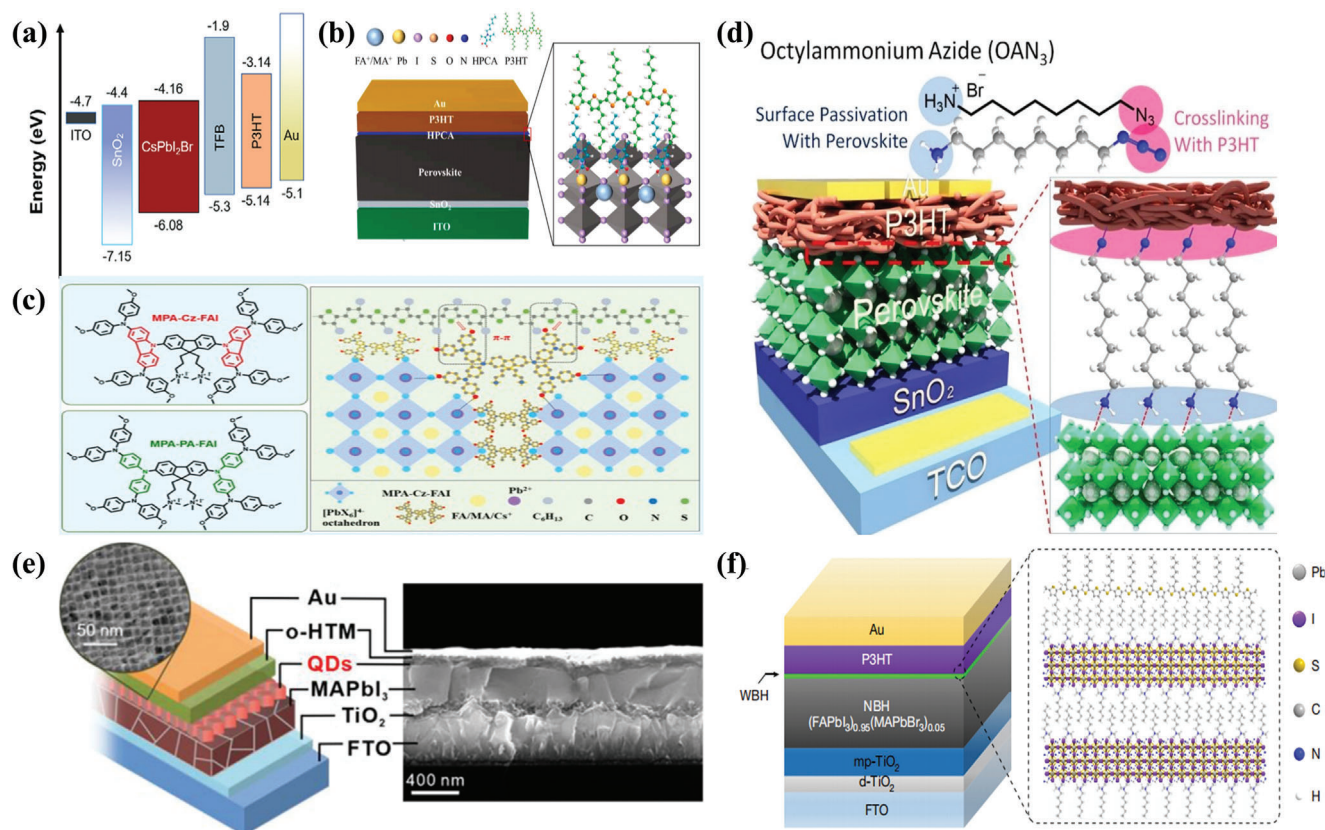


Figure 3. a) Schematic energy level alignment of CsPbI₂Br PSC with TFB interlayer. Reproduced with permission.^[66] Copyright 2020, John Wiley and Sons. b) The device structure of planar heterojunction PSCs, and possible interaction between HPCA, perovskite, and P3HT. Reproduced with permission.^[69] Copyright 2022, Elsevier. c) MPA-Cz-FAI and MPA-PA-FAI molecular structure and schematic diagram and working mechanism of MPA-Cz-FAI between perovskite and P3HT macromolecular. Reproduced with permission.^[70] Copyright 2023, American Chemical Society. d) Schematic illumination of PSCs with cross-linkable molecule, OAN₃. Reproduced with permission.^[71] Copyright 2023, Royal Society of Chemistry. e) Schematic of PSCs structure and representative TEM image of CsPbI_{1.85}Br_{1.15} QDs and cross-section SEM image of device structure based on P3HT with QDs interlayer. Reproduced with permission.^[73] Copyright 2021, American Chemical Society. f) The structure of an n-i-p PSCs based on DHA using P3HT as HTM and schematic structure of the interface between the WBH and P3HT. Reproduced with permission.^[74] Copyright 2019, Springer Nature.

P3HT-based PSCs appeared in 2019 when a double-layered halide architecture (DHA) was proposed by Seo et al. By spin-coating n-hexyl trimethyl ammonium bromide (HTAB) onto the perovskite surface, a wide-bandgap halide layer was constructed between the perovskite absorbing layer and P3HT which can induce the self-assembly of P3HT and simultaneously enhance the van der Waals interactions between perovskite and P3HT. Furthermore, HTAB plays a role in reducing recombination at perovskite interfaces, thereby enhancing the lifetime of carriers in perovskite. Consequently, the interfacial non-radiative recombination was significantly reduced and a record PCE of 23.3% was realized along with an overall enhanced device stability (Figure 3f).^[74]

3.3. Morphology Control in P3HT-Based PSCs

It is well known that the film morphology of conjugated polymers is closely related to the chemical structure of polymeric monomer, MW, solubility, conformational distribution as well as the method of deposition.^[75,76] For regioregular P3HT, the

simple thiophene monomer and hexyl side chain endow it with good solubility and high freedom to sample conformational space, hence the polymer morphology is mainly dependent on the MW and the technique of deposition. Generally, P3HT is a highly aggregated semicrystalline material in the solid state which is distinct from the amorphous morphology of PTAA.^[77] P3HT tends to form a unique packing motif in which folded chains assume needle-like crystallites with the π -stacking axis parallel to the long axis of the crystallite, leading to fibrillar shapes in the film state.^[78] However, the degree of crystallization and the nanofiber alignment are different depending on the MW of P3HT and deposition techniques.^[32] For example, drop casting or dip casting with the slower evaporation of solvent can induce more ordered arrangements in P3HT which usually form an edge-on orientation with respect to the underlying surface, while spin casting with a fast evaporation of solvent may lead to less ordered structures in which the specific arrangement of P3HT relies on various parameters such as the regioregularity,^[79] MW,^[80] the solvent,^[81] the speed of spinning^[82] as well as the surface properties of the substrate.^[83] Further, the alignment of P3HT nanofibers can also be

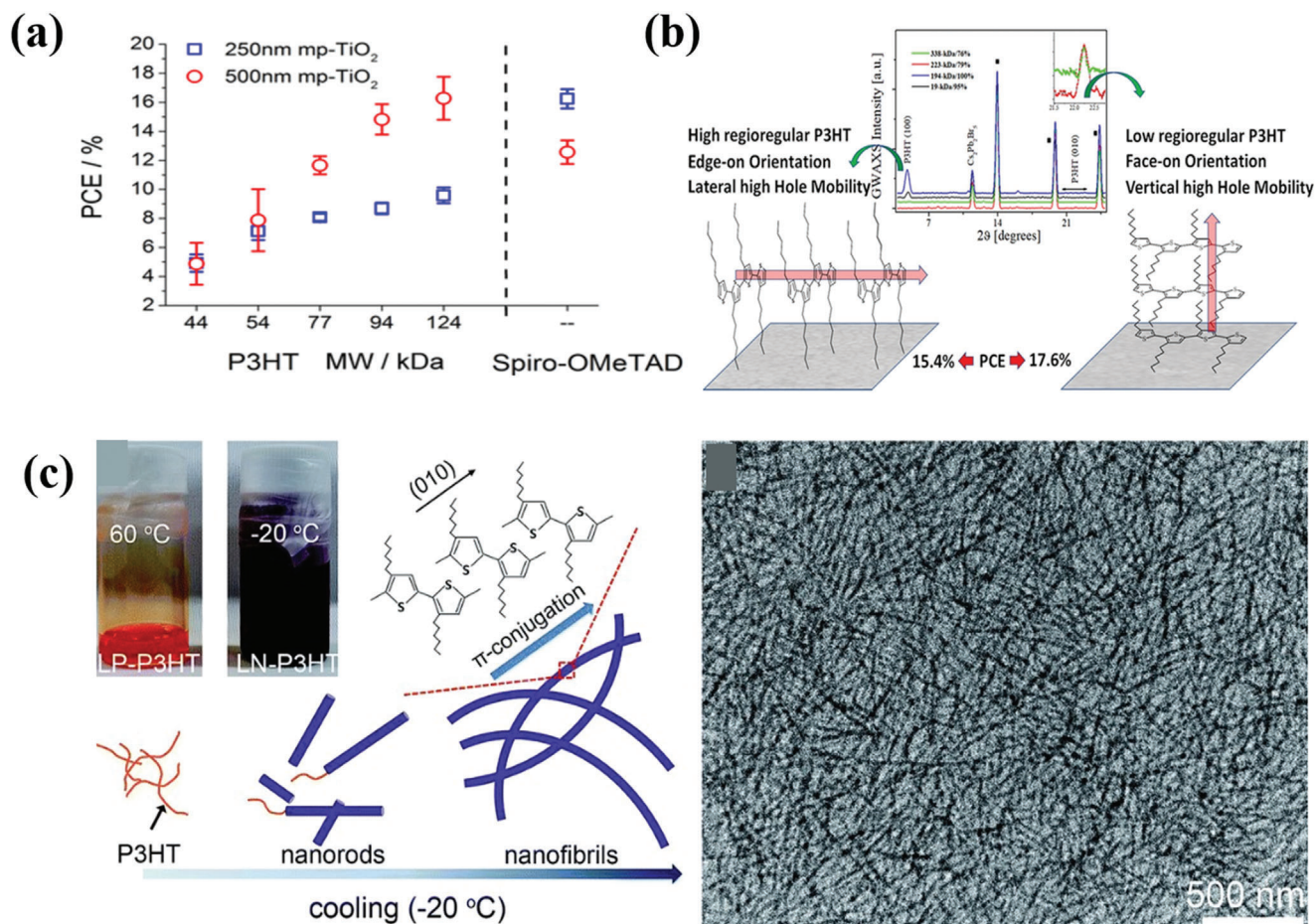


Figure 4. a) Schematic illumination of efficiency enhancement is mainly related to the increase of J_{sc} and FF as P3HT MW increases. Reproduced with permission.^[89] Copyright 2017, John Wiley and Sons. b) GIWAXS patterns of glass/FTO/perovskite/P3HT samples and working mechanism of P3HT stacking orientation. Reproduced with permission.^[90] Copyright 2021, American Chemical Society. c) Schematic of the growth mechanism of the LN-P3HT during the low cooling process and TEM image of the as-spun LN-P3HT thin film. Reproduced with permission.^[91] Copyright 2016, Royal Society of Chemistry.

regulated using different processing or deposition strategies such as flow-aligned crystallization,^[84] preassembly in solution,^[85] sonication,^[86] and UV irradiation.^[87] Collectively, the alteration of film morphology of P3HT mainly lies on the MW and processing method which will profoundly affect the electronic properties of P3HT as well as the interfacial contact between P3HT and perovskite.

Di Carlo et al. performed a systematic study on the effect of the MW of P3HT on the performance of PSCs by varying the P3HT MW from 44 to 124 kDa. The results show that the larger MW contributes to the higher efficiency which can be attributed to two factors: i) the increased MW of P3HT is beneficial for enhancing the interfacial charge-transfer resistance, that is, reducing the interfacial recombination of free charges; ii) P3HT with higher MW possesses higher absorption coefficient due to the strengthened chain-chain interactions^[88] which provides an additional contribution to the external quantum efficiency (EQE) of PSCs. Therefore, the highest PCE of 16.2% was achieved by P3HT-based PSCs with a MW of 124 kDa (Figure 4a).^[89] Further, the same group developed a series of P3HT with different MWs

and regioregularities (RRs) following different synthetic routes. It was found that P3HT films with higher RR and lower MW prefer to exhibit an edge-on configuration while the lower RR combined with higher MW promotes a face-on configuration. Although the RR affects the crystallinity and orientation of P3HT films, the higher MW accounted in general for the better device performance and reproducibility since it gives smooth and pinhole-free films, especially for large-area devices where 16.7% PCE (6.25 cm²) was obtained based on the highest MW P3HT (338 kDa) (Figure 4b).^[90]

The well-controlled crystallinity and morphology of P3HT also render great potential for flexible applications. By employing a rapid cooling process of P3HT solutions in *m*-xylene, Park et al. yielded long P3HT nanofibrils with high crystallinity. Compared to the control P3HT film, the newly prepared P3HT film exhibits more efficient hole extraction and a lower specific contact resistivity to the Au electrode as well as higher air stability, all of which contribute to the successful fabrication of large-area flexible PSCs with 13.12% efficiency (1 cm²) (Figure 4c).^[91]

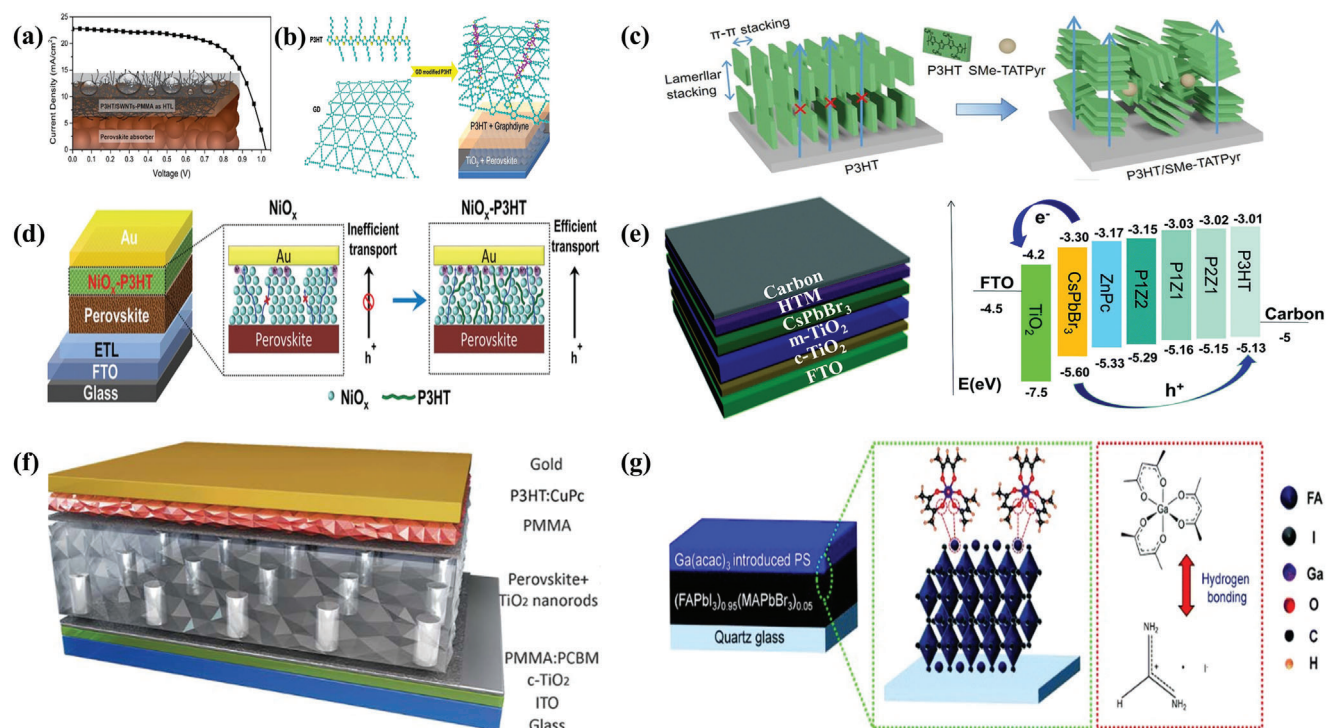


Figure 5. a) Schematic of the P3HT/SWNTs-PMMA as HTM. Reproduced with permission.^[95] Copyright 2014, American Chemical Society. b) Schematic diagram of the PSCs with P3HT HTM modified with graphdiyne. Reproduced with permission.^[96] Copyright 2015, John Wiley and Sons. c) Schematic diagram of the SMe-TATPy manipulating P3HT stacking. Reproduced with permission.^[98] Copyright 2021, John Wiley and Sons. d) Schematic illustration of the device structure and the engineering effect of NiO_x-based HTM. Reproduced with permission.^[100] Copyright 2022, John Wiley and Sons. e) Schematic diagram of the PSCs device structure and energy level diagram of solar cell materials in the PSC. Reproduced with permission.^[102] Copyright 2019, Royal Society of Chemistry. f) Schematic of nanopattern PSC device structure. Reproduced with permission.^[103] Copyright 2021, The American Association for the Advancement of Science. g) Schematic illustration of the Ga(acac)₃ behavior on the perovskite surface. Reproduced with permission.^[27] Copyright 2021, Royal Society of Chemistry.

3.4. Formation of Composite HTMs in P3HT-Based PSCs

Although P3HT features good charge mobility in the pristine film, it is highly associated with the established film morphology which is sometimes difficult to optimize, especially for the deposition on the soft structure of the perovskite layer. On the other hand, the oxidability of thiophene unit is less active than phenylamine moiety. Hence, a doping strategy is sometimes utilized to enhance the hole conductivity of P3HT. It was found that by doping with either lithium salt,^[92] cobalt complex^[93] or F4-TCNQ,^[94] the hole-transporting capacity of P3HT could be significantly enhanced alongside the downshifted HOMO level. Therefore, efficient hole extraction and transfer and inhibited trap-assisted recombination could be anticipated, resulting in enhanced device efficiency. However, the dopants, especially for those with high redox properties or hygroscopicity, may undoubtedly jeopardize the device stability during the long operation time due to ion migration, phase segregation, and water intrusion. To address this issue, designing rational composite HTMs to optimize the properties of P3HT is envisioned as a promising alternative.

Early in 2014, Snaith et al. combined P3HT, single-walled carbon nanotubes (SWNTs), and insulating polymer PMMA to form a stable composite HTM structure that achieves competitive PCE of 15.3% and importantly, offers unprece-

ded resilience against thermal stressing and moisture ingress (Figure 5a).^[95] Similar to SWNTs, another 2D carbon material, graphdiyne (GD) with large π -conjugation, was incorporated into P3HT by Li et al. to strengthen intermolecular π - π interactions and facilitate interfacial charge transfer. As a consequence, a comparable PCE of 14.58% was achieved based on MAPbI₃ perovskite (Figure 5b).^[96] Similarly, the functionalized graphene can be also employed to modify the hole mobility and energy level of P3HT which enables 13.82% efficiency of PSCs.^[97]

Apart from carbon materials, organic species with fine-tuned structures and properties can assist in the modification of P3HT. Hu et al. designed a conjugated small molecule namely SMe-TATPy to manipulate the morphology of P3HT film. It was found that the composite P3HT/SMe-TATPy HTM shows nearly an order of magnitude increase of carrier mobility from $3.43 \times 10^{-3} \text{ cm}^2 \text{ V}^{-1} \text{ s}^{-1}$ for pristine P3HT to $1.01 \times 10^{-2} \text{ cm}^2 \text{ V}^{-1} \text{ s}^{-1}$ which is due to the breaking of the long-range ordering of "edge-on" P3HT domains and simultaneously the formation of "face-on" clusters. Moreover, the composite HTM features favorable energy level alignment with CsPbI₂Br perovskite and enables reduced perovskite surface defect density, which contributes to reduced voltage loss and a resultant high PCE of 16.93% with a V_{oc} of 1.38 V. Crucially, the device shows superior moisture and thermal stability with

maintaining 96% efficiency for 1500 h under RH of 25% and over 95% efficiency after annealing at 85 °C for 1000 h (Figure 5c).^[98] Gao et al. constructed a multifunctional molecule namely 2-((7-(4-(bis(4-methoxyphenyl)amino)phenyl)-10-(2-(2-ethoxyethoxy)ethyl)-10H-phenoxazin-3-yl)methylene)malononitrile (MDN) whose malononitrile group can anchor the perovskite surface while the triphenylamine group can form π - π stacking with P3HT to form a charge transport channel. Also, MDN can effectively passivate the defects and largely reduce the interfacial recombination. Consequently, a considerably high PCE of 22.87% was achieved with MDN-doped P3HT as HTM, much higher than that based on pristine P3HT (12.48%). Importantly, the unencapsulated device exhibits excellent long-term stability with 92% of initial efficiency maintained even after 2 months of aging at 75% RH followed by 1-month of aging at 85% RH in the atmosphere.^[99]

By mixing inorganic metal oxide nickel oxide (NiO_x) into P3HT reported by Wu et al., the synergistic interaction between NiO_x and P3HT could take place, that is, P3HT assists assembly regularity and film uniformity of NiO_x and conversely, NiO_x enhances molecular orientation of polymer chains in P3HT. As a result, enhanced hole transport was obtained in hybrid NiO_x and P3HT HTM, and the corresponding PCE was synchronously improved from 16.0% to 21.2%. Note that after 1000 h aging at a harsh 85 °C/85% RH condition, the encapsulated PSC modules ($6 \times 6 \text{ cm}^2$) can maintain 91% of the original efficiency (Figure 5d).^[100] Xu et al. demonstrated that plasmonic gold nanorods (AuNRs) are propitious for enhancing the crystallinity of P3HT and the resultant hole mobility. In addition, AuNRs can help to increase the light utilization of PSCs. Therefore, P3HT/AuNRs composite HTM facilitates the device PCE to 16.88%, which is an increase of 26% compared to that based on pristine P3HT (13.40%).^[101]

Metal complex is another type of semiconductor with simple synthesis, fine-tuned energy level, and high thermal and chemical stability. He et al. incorporated zinc phthalocyanine (ZnPc) into P3HT by changing their mass ratios to tailor the energy level of P3HT in order to match well with that of CsPbBr_3 perovskite. When using carbon as the electrode, the PSCs based on P3HT/ ZnPc composite show an appealing PCE of 10.03% (Figure 5e).^[102] Similarly, copper phthalocyanine (CuPc) was utilized by White et al. as a modulator to induce highly crystalline P3HT film with enhanced hole conductivity. Accompanied by introducing a nanopatterned electron transport layer of TiO_2 , the PSCs achieved a remarkably high PCE of 23.17% and notably a certified PCE of 21.6% for a 1-square-centimeter device with a high FF of 0.839 (Figure 5f).^[103] Coincidentally, Noh et al. reported a gallium(III) acetylacetonate ($\text{Ga}(\text{acac})_3$) as a modulator in P3HT in the same year. The key contribution of $\text{Ga}(\text{acac})_3$ is to passivate the defects of the perovskite surface through hydrogen bonding between the $\text{Ga}(\text{acac})_3$ and organic cation and optimize the junction quality at the perovskite/P3HT interface so that the interfacial recombination loss can be significantly reduced. Furthermore, the double-layered halide architecture (DHA) strategy was additionally implemented to boost the PCE to 24.6% which is the highest efficiency value reported to date for P3HT-based PSCs (Figure 5g).^[27]

3.5. Modification of P3HT and Derived Applications

3.5.1. Chemical Modification of P3HT

As reviewed in Section 2, traditional P3HT is produced by using 2,5-dibromo-3-hexylthiophene monomers through the Grignard metathesis method. Although the molecular weight and film morphology could be fine-tuned via the synthetic or post-treatment method, the chemical functionality is limited due to the simple structure of the thiophene monomer. With the premise that the synthetic route is low-cost and uncomplicated, modification of P3HT through molecular backbone or side chains is a feasible way to enhance the functionalities of P3HT so as to render tunable electrical, morphological, and interfacial properties to P3HT, which may provide guidance for the applications of P3HT derivatives in PSCs.^[104] For example, Chen et al. altered the P3HT terminal with electron-deficient groups such as oxadiazole (OXD) and triazole (TAZ), which can result in enhanced absorption coefficient, prolonged exciton lifetime, and improved chain ordering for carrier transport (Figure 6a).^[105] Thompson et al. reported a kind of poly(3-hexylthiophene)-based random copolymers with distinct surface energy featuring either an oligoether (P3HT-*co*-MET) or semifluoroalkyl (P3HT-*co*-FHT) side chain (Figure 6b).^[106] Compared to P3HT (19.9 mN m^{-1}), the semifluoroalkyl side chain can reduce the surface energy (14.2 mN m^{-1}), while the oligoether side chain is able to enhance the surface energy (27.0 mN m^{-1}). Yokozawa et al. explored a post-end-modification method, i.e., Sonogashira coupling of P3HT having H/Br ends with trimethylsilylacetylene, followed by removal of the trimethylsilyl group, instead of the traditional ethynylmagnesium chloride-quenching method, which can afford exclusively P3HT with an ethynyl group at one end and subsequent well-controlled diblock copolymer. This ethynylation method may be useful for postfunctionalization of P3HT via forming well-defined diblock copolymers (Figure 6c).^[107] Also, Swager et al. put forward a facile postpolymerization modification strategy to functionalize the 4-position of P3HT incorporating lithium-bromine exchange and quenching with an electrophile. The functional electrophiles can produce different P3HT derivatives with distinct properties (Figure 6d).^[108]

3.5.2. Derived Applications

Perovskite materials possess a soft crystalline structure that enhances their resilience to stress variations, making them suitable for the fabrication of flexible PSCs.^[109] Meanwhile, the intrinsic flexibility of polymeric materials such as P3HT is also suitable for constructing flexible devices. The first flexible PSC based on dopant-free P3HT was reported by Lu et al. in 2015 with a 7.2% PCE and can retain 61% of its initial efficiency after 50 bending cycles.^[59] Liu et al. utilized high-bending graphene electrodes to realize ultraflexible PSCs with P3HT as HTM, achieving 11.5% PCE with an output power of 5.07 W per gram.^[110] When incorporating p-dopants to enhance the hole extraction capability of P3HT, the resultant PSCs on flexible substrates can achieve a PCE of 11.84% with good mechanical durability (more than 93% of initial PCE was retained after 600 bending cycles at 10 mm curvature).^[93] Recently, Seo et al. reported roll-to-roll

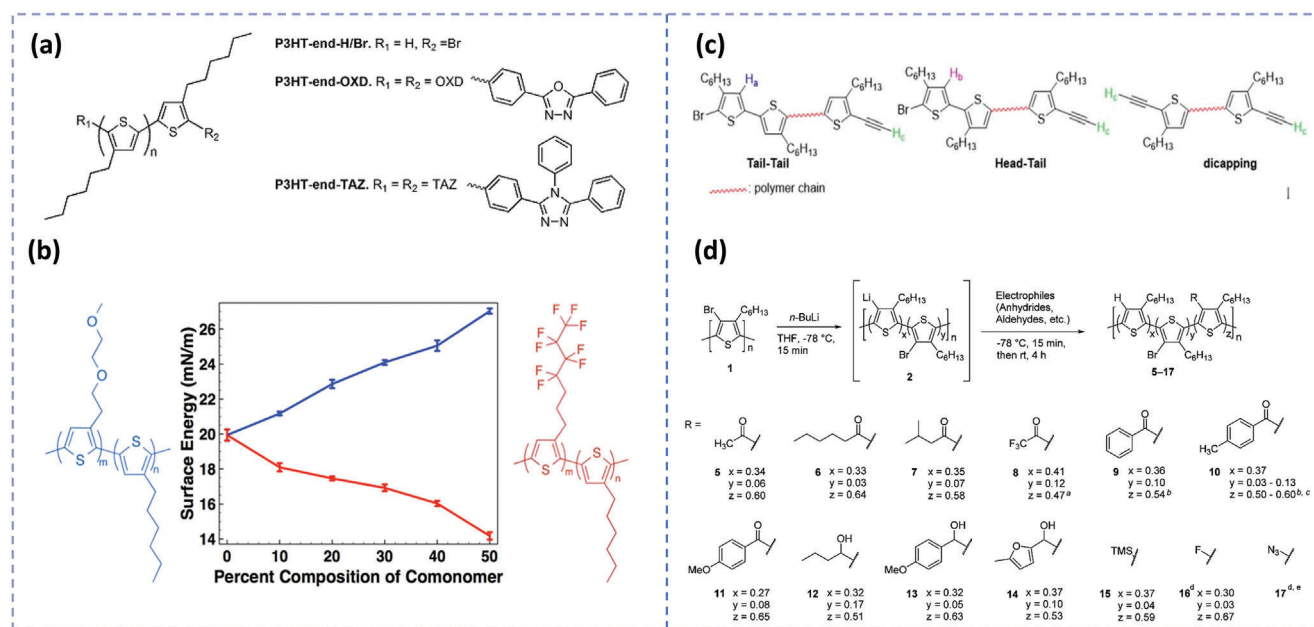


Figure 6. a) Configuration of P3HT and associated alterations to end-groups. Reproduced with permission.^[105] Copyright 2015, American Chemical Society. b) The surface energy of P3HT-co-MET (blue) and P3HT-co-FHT (blue) as-cast thin films. Reproduced with permission.^[106] Copyright 2015, American Chemical Society. c) Three kinds of end-terminal groups P3HT after quenching with ethynyl magnesium chloride. Reproduced with permission.^[107] Copyright 2018, John Wiley and Sons. d) Polymerisation modification and quenching of electrophilic reagents after lithium-bromine exchange. Reproduced with permission.^[108] Copyright 2014, American Chemical Society.

gravure-printed flexible PSCs using eco-friendly antisolvent and realized the recorded PCE of 13.8% for fully roll-to-roll-produced flexible PSCs using P3HT as an HTM.^[111]

In order to facilitate the commercialization of PSCs, the fabrication of large-area modules with high performance is essentially important. P3HT has proven to be suitable for various solution-processing techniques such as slot-die coating and roll-to-roll printing. The first work on a large-area PSC with doped P3HT as an HTM was reported by Matteocci et al. which shows a high PCE of 8.2% for devices with 10.08 cm² active area.^[112] Based on this work, Razza et al. used air-assisted blade coating of PbI₂ for large-scale PSCs with 4.3% PCE for a 100 cm² module for the first time.^[113] By using a thin wide-bandgap halide perovskite approach, Jung et al. reported a high PCE of 17.1% for P3HT-based PSCs with a 24.97 cm² module.^[74] For an even larger area, Ren et al. reported a 50 cm² fully printed module achieving a high 17.05% PCE.^[114]

4. Conclusion and Outlook

As the most promising candidate for next-generation photovoltaic technology, the PSCs have experienced leapfrog development over the past few years which is moving close to the brink of commercialization. To push the PSCs toward an industrial scale, cost analysis, and operational stability should be highly stressed apart from device efficiency. It was assessed that the HTMs constitute a major portion of the fabrication cost of PSC modules, i.e., nearly half of the total raw material cost^[115], especially for n-i-p PSCs. Due to the inherent instability of widely-used Spiro-OMeTAD and PTAA as doped HTMs and the low efficiency or universality of recently-developed dopant-free HTMs, exploring

low-cost and highly stable HTMs with both high efficiency and superior universality is an imminent need at the current stage. Fortunately, benefiting from the long-term research on classical organic semiconductors, P3HT has experienced a renaissance during the past decade as a feasible candidate for HTMs in PSCs. P3HT consists of simple repeating monomer 3-hexylthiophene and can be synthesized easily with low cost and excellent control over MW, polydispersity index, and regioregularity^[116,117] which make it one of the few polymers available in bulk quantities with excellent batch-to-batch purity.^[118] Moreover, P3HT has good thermal, chemical, and electrochemical stability and its high crystallinity enables the formation of aligned molecular configurations and the resultant high hole mobility in the solid state.^[119] Additionally, the hydrophobicity of P3HT can interdict the moisture penetration which is favorable for enhancing the humidity stability of PSCs. Despite this, the pivotal deficiency associated with P3HT-based PSCs is the device efficiency which is still constrained below 25%. The main culprit for the lagged PCE consists of the mismatched energy level of P3HT with perovskite and the poor interfacial contact between P3HT and perovskite which may lead to poor charge extraction and severe nonradiative recombination. Hence, in this review, we fully summarize the developed strategies to address the issues related to P3HT-based PSCs including interface engineering, morphology control in the bulk film of P3HT, and the design of composite HTMs involving P3HT, which indeed assist the enhancement of PCE in P3HT-based PSCs as compared to the initial report in 2013. However, there is still much room for further improvement of P3HT-based PSCs either from material design or from device optimization. Here, some guidelines and outlooks toward future research are pointed out as follows:

i. Material design

The interfacial contact between P3HT and perovskite is the key issue that limits the device performance of P3HT-based PSCs. When designing proper interfacial modulators, several factors such as energy level alignment, surface dipoles, chemical interactions, and oxygen/water barriers should be taken into consideration. Generally, from the viewpoint of molecular design, various chemical strategies could be adopted to regulate the functionalities of materials. For example, donor–acceptor framework,^[120] fluorination strategy,^[121] and push-pull functional groups^[122] can be utilized to tune molecular energy levels, while side-chain engineering,^[123] counterions^[124] and zwitterionic structure^[125] are propitious for tailoring surface dipoles and hydrophobicity. Moreover, the introduction of specific functional groups such as Lewis base groups is deemed to passivate the defects of the perovskite surface.^[126] Hence, integrating these desired properties into a single material as an efficient interfacial modulator seems promising but challenging in future research work.

Besides the design of interfacial molecules, the efficient composite materials that can tune the morphology and electronic properties of P3HT film need to be explored. It is known that there is a trade-off between the interfacial contact and charge transport ability, that is, high crystallinity of HTMs is appraisive for enhancing charge mobility but sometimes leads to poor interfacial contact and adhesion, while the amorphous HTMs usually show controllable surface properties but poor intrinsic conductivity.^[127–129] Since P3HT tends to form highly oriented film with nanofiber-like crystal domains, the interfacial contact between P3HT and perovskite is confirmed to be injurious for hole transfer at the interface.^[130] Also, it was revealed that the conductivity of P3HT is not the main limiting parameter of the corresponding PSCs.^[130] In this regard, it is viable to mix proper components with P3HT to optimize the interfacial contact between P3HT and perovskite despite the possibility of jeopardizing the intrinsic hole mobility of P3HT. Due to the complexity of the film assembly of composite HTMs, it necessitates intensive efforts to rationally design various material systems to uncover the role and mechanism of blending components in regulating the morphology, electronic properties, and interfacial properties of P3HT.

Alternatively, to avoid the usage of additional components in the hole-transporting layer, the marginal alteration of P3HT itself could be performed by exchanging the substitution groups with ester groups or halogen atoms to endow polythiophenes with optimized electronic and morphological properties at the molecular level. In fact, such P3HT derivatives have been explored as donor polymers in organic solar cells which show even outperforming device performance compared to P3HT.^[131,132] With the premise that these polythiophenes possess low-cost synthesis and fine controllable MW and polydispersity index, their applications in PSCs as efficient HTMs may be anticipated.

ii. Device optimization

Apart from material design, much attention should be paid to device optimization in future work regarding each functional layer. For P3HT-based PSCs, the perovskite active layer, P3HT layer, electrode, and the interfaces between them are crucial to

the final device efficiency. The reported methods for perovskite engineering could be tested to obtain a high-quality perovskite layer with suitable surface adjacent to P3HT film. Also, interface engineering involving structure regulation such as double-layered halide architecture,^[74] dimensionality engineering,^[133] and crosslinked quantum well^[134] is conducive to reducing the charge recombination at the interface, eliminating the interfacial defects and favoring the hole transfer from perovskite to P3HT. As for P3HT layer, the morphology control is the most important link which can be tuned by various processing techniques as found in the previous reviews.^[32,135] Additionally, the selection of electrodes may affect the overall device performance, stability, and cost to a large extent. For example, carbon electrodes are low-cost, stable, and compatible with large-scale production which has shown great potential in achieving highly stable P3HT-based PSCs either in normal or indoor applications.^[136,137] Another low-cost copper electrode, which has been successfully applied in conventional PSCs,^[138,139] can also be tried to place in P3HT-based PSCs. In many research works on dopant-free HTMs, molybdenum oxide (MoO_x) is usually adopted between HTM and electrode which can not only block electron flux but also act as interfacial p-dopant to enhance hole transfer from HTM to electrode.^[140,141] This strategy may be equally useful in P3HT-based PSCs.

Finally, the large-area flexible PSCs are envisioned as promising photovoltaic technology to promote a new generation of soft electronics and machines requiring high power-per-weight.^[142] Due to the inherent merit of polymeric P3HT, its solution with certain viscosity is applicative to the large-area roll-to-roll printing or inkjet printing process which is favorable for the cost reduction in the practical production. Moreover, the polymeric P3HT or the corresponding composites feature plastic and scalable characteristics which are variable and controllable toward application in flexible devices. Therefore, more efforts should be devoted to the fabrication and investigation of large-area flexible PSCs using P3HT HTM in future work. In summary, with the development of material design and device optimization, it is believed that P3HT may play a remarkably promising role on the road to industrialization of PSCs, and it is hoped that this review can provide an overview of the recent progress on P3HT as a HTM utilized in PSCs and cast light on the future research momentum in the P3HT-based PSCs.

Acknowledgements

This work was supported by the National Natural Science Foundation of China (52203228), Fujian Province Natural Science Foundation of China (2023J01527), Natural Science Foundation of Guangdong Province of China (2023A1515011916), and the Start-up funding from Fujian Normal University (Y0720312K13).

Conflict of Interest

The authors declare no conflict of interest.

Keywords

hole-transporting materials, P3HT, perovskite solar cells, stability

Received: February 2, 2024
Revised: May 14, 2024
Published online: May 25, 2024

- [1] M. A. Green, S. P. Bremner, *Nat. Mater.* **2017**, *16*, 23.
- [2] V. Fthenakis, *Renew. Sustain. Energy Rev.* **2009**, *13*, 2746.
- [3] A. Hagfeldt, G. Boschloo, L. Sun, L. Kloo, H. Pettersson, *Chem. Rev.* **2010**, *110*, 6595.
- [4] Y. Cui, Y. Xu, J. Hou, *Sci. Bull.* **2022**, *67*, 1300.
- [5] W. Fu, L. Wang, J. Ling, H. Li, M. Shi, J. Xue, H. Chen, *Nanoscale* **2014**, *6*, 10545.
- [6] A. K. Jena, A. Kulkarni, T. Miyasaka, *Chem. Rev.* **2019**, *119*, 3036.
- [7] M. I. Hossain, A. M. Saleque, S. Ahmed, I. Saidjafarzoda, Md. Shahiduzzaman, W. Qarony, D. Knipp, N. Biyikli, Y. H. Tsang, *Nano Energy* **2021**, *79*, 105400.
- [8] M. Jošt, L. Kegelmann, L. Korte, S. Albrecht, *Adv. Energy Mater.* **2020**, *10*, 1904102.
- [9] R. Wang, T. Huang, J. Xue, J. Tong, K. Zhu, Y. Yang, *Nat. Photonics* **2021**, *15*, 411.
- [10] J. Zhu, Y. Luo, R. He, C. Chen, Y. Wang, J. Luo, Z. Yi, J. Thiesbrummel, C. Wang, F. Lang, H. Lai, Y. Xu, J. Wang, Z. Zhang, W. Liang, G. Cui, S. Ren, X. Hao, H. Huang, Y. Wang, F. Yao, Q. Lin, L. Wu, J. Zhang, M. Stollerfoht, F. Fu, D. Zhao, *Nat. Energy* **2023**, *8*, 714.
- [11] NREL, Best Research-Cell Efficiencies, https://www.nrel.gov/ncpv/images/efficiency_chart.jpg (accessed: January 2024).
- [12] U. Bach, D. Lupo, P. Comte, J. E. Moser, F. Weissörtel, J. Salbeck, H. Spreitzer, M. Grätzel, *Nature* **1998**, *395*, 583.
- [13] F. E. Goodson, S. I. Hauck, J. F. Hartwig, *J. Am. Chem. Soc.* **1999**, *121*, 7527.
- [14] D. Khan, X. Liu, G. Qu, A. R. Nath, P. Xie, Z. Xu, *Small* **2023**, *19*, 2205926.
- [15] X. Sun, X. Yu, Z. Li, *ACS Appl. Energy Mater.* **2020**, *3*, 10282.
- [16] W. Chen, Y. Wang, B. Liu, Y. Gao, Z. Wu, Y. Shi, Y. Tang, K. Yang, Y. Zhang, W. Sun, X. Feng, F. Laquai, H. Y. Woo, A. B. Djurišić, X. Guo, Z. He, *Sci. China Chem.* **2021**, *64*, 964.
- [17] Y. Ren, M. Ren, X. Xie, J. Wang, Y. Cai, Y. Yuan, J. Zhang, P. Wang, *Nano Energy* **2021**, *81*, 105655.
- [18] M. De Bastiani, V. Larini, R. Montecucco, G. Grancini, *Energy Environ. Sci.* **2023**, *16*, 421.
- [19] Z. Bao, A. Dodabalapur, A. J. Lovinger, *Appl. Phys. Lett.* **1996**, *69*, 4108.
- [20] F. Padinger, R. S. Rittberger, N. S. Sariciftci, *Adv. Funct. Mater.* **2003**, *13*, 85.
- [21] W. U. Huynh, J. J. Dittmer, A. P. Alivisatos, *Science* **2002**, *295*, 2425.
- [22] B. Xu, S. Holdcroft, *Macromolecules* **1993**, *26*, 4457.
- [23] P. Schilinsky, C. Waldauf, C. J. Brabec, *Appl. Phys. Lett.* **2002**, *81*, 3885.
- [24] U. Mehmood, A. Al-Ahmed, I. A. Hussein, *Renew. Sustain. Energy Rev.* **2016**, *57*, 550.
- [25] A. T. Kleinschmidt, S. E. Root, D. J. Lipomi, *J. Mater. Chem. A* **2017**, *5*, 11396.
- [26] D. Bi, L. Yang, G. Boschloo, A. Hagfeldt, E. M. J. Johansson, *J. Phys. Chem. Lett.* **2013**, *4*, 1532.
- [27] M. J. Jeong, K. M. Yeom, S. J. Kim, E. H. Jung, J. H. Noh, *Energy Environ. Sci.* **2021**, *14*, 2419.
- [28] H. Shirakawa, T. Ito, S. Ikeda, *Polym. J.* **1973**, *4*, 460.
- [29] T. A. Chen, R. D. Rieke, *J. Am. Chem. Soc.* **1992**, *114*, 10087.
- [30] R. D. McCullough, R. D. Lowe, M. Jayaraman, D. L. Anderson, *J. Org. Chem.* **1993**, *58*, 904.
- [31] R. D. McCullough, S. Tristram-Nagle, S. P. Williams, R. D. Lowe, M. Jayaraman, *J. Am. Chem. Soc.* **1993**, *115*, 4910.
- [32] M. T. Dang, L. Hirsch, G. Wantz, J. D. Wuest, *Chem. Rev.* **2013**, *113*, 3734.
- [33] S. Savagatrup, A. D. Printz, H. Wu, K. M. Rajan, E. J. Sawyer, A. V. Zaretski, C. J. Bettinger, D. J. Lipomi, *Synth. Met.* **2015**, *203*, 208.
- [34] S. Savagatrup, A. D. Printz, T. F. O'Connor, A. V. Zaretski, D. Rodriguez, E. J. Sawyer, K. M. Rajan, R. I. Acosta, S. E. Root, D. J. Lipomi, *Energy Environ. Sci.* **2015**, *8*, 55.
- [35] C. Zhang, K. Wei, J. Hu, X. Cai, G. Du, J. Deng, Z. Luo, X. Zhang, Y. Wang, L. Yang, J. Zhang, *Mater. Today* **2023**, *67*, 518.
- [36] M. A. Haque, A. D. Sheikh, X. Guan, T. Wu, *Adv. Energy Mater.* **2017**, *7*, 1602803.
- [37] P. Murugan, T. Hu, X. Hu, Y. Chen, *J. Mater. Chem. A* **2022**, *10*, 5044.
- [38] X. Wang, M. Wang, Z. Zhang, D. Wei, S. Cai, Y. Li, R. Zhang, L. Zhang, R. Zhang, C. Zhu, X. Huang, F. Gao, P. Gao, Y. Wang, W. Huang, *Research* **2024**, *7*, 0332.
- [39] J. Salbeck, N. Yu, J. Bauer, F. Weissörtel, H. Bestgen, *Synth. Met.* **1997**, *91*, 209.
- [40] H.-S. Kim, C.-R. Lee, J.-H. Im, K.-B. Lee, T. Moehl, A. Marchioro, S.-J. Moon, R. Humphry-Baker, J.-H. Yum, J. E. Moser, M. Grätzel, N.-G. Park, *Sci. Rep.* **2012**, *2*, 591.
- [41] Z. Hawash, L. K. Ono, Y. Qi, *Adv. Mater. Inter.* **2018**, *5*, 1700623.
- [42] J. Park, J. Kim, H.-S. Yun, M. J. Paik, E. Noh, H. J. Mun, M. G. Kim, T. J. Shin, S. I. Seok, *Nature* **2023**, *616*, 724.
- [43] Z. Huang, Y. Bai, X. Huang, J. Li, Y. Wu, Y. Chen, K. Li, X. Niu, N. Li, G. Liu, Y. Zhang, H. Zai, Q. Chen, T. Lei, L. Wang, H. Zhou, *Nature* **2023**, *623*, 531.
- [44] S.-Y. Jeong, H.-S. Kim, N.-G. Park, *ACS Appl. Mater. Interfaces* **2022**, *14*, 34220.
- [45] M. V. Khenkin, E. A. Katz, A. Abate, G. Bardizza, J. J. Berry, C. Brabec, F. Brunetti, V. Bulović, Q. Burlingame, A. Di Carlo, R. Cheacharoen, Y.-B. Cheng, A. Colmann, S. Cros, K. Domanski, M. Duszka, C. J. Fell, S. R. Forrest, Y. Galagan, D. Di Girolamo, M. Grätzel, A. Hagfeldt, E. Von Hauff, H. Hoppe, J. Kettle, H. Köbler, M. S. Leite, S. Liu, Y.-L. Loo, J. M. Luther, et al., *Nat. Energy* **2020**, *5*, 35.
- [46] J. H. Heo, S. H. Im, J. H. Noh, T. N. Mandal, C.-S. Lim, J. A. Chang, Y. H. Lee, H. Kim, A. Sarkar, Md. K. Nazeeruddin, M. Grätzel, S. I. Seok, *Nat. Photonics* **2013**, *7*, 486.
- [47] W. S. Yang, B.-W. Park, E. H. Jung, N. J. Jeon, Y. C. Kim, D. U. Lee, S. S. Shin, J. Seo, E. K. Kim, J. H. Noh, S. I. Seok, *Science* **2017**, *356*, 1376.
- [48] F. M. Rombach, S. A. Haque, T. J. Macdonald, *Energy Environ. Sci.* **2021**, *14*, 5161.
- [49] Y. Wang, W. Chen, L. Wang, B. Tu, T. Chen, B. Liu, K. Yang, C. W. Koh, X. Zhang, H. Sun, G. Chen, X. Feng, H. Y. Woo, A. B. Djurišić, Z. He, X. Guo, *Adv. Mater.* **2019**, *31*, 1902781.
- [50] Q. Cheng, H. Chen, F. Yang, Z. Chen, W. Chen, H. Yang, Y. Shen, X. Ou, Y. Wu, Y. Li, Y. Li, *Angew. Chem. Int. Ed.* **2022**, *61*, 202210613.
- [51] Y. Wang, Q. Liao, J. Chen, W. Huang, X. Zhuang, Y. Tang, B. Li, X. Yao, X. Feng, X. Zhang, M. Su, Z. He, T. J. Marks, A. Facchetti, X. Guo, *J. Am. Chem. Soc.* **2020**, *142*, 16632.
- [52] Y. Bai, Z. Zhou, Q. Xue, C. Liu, N. Li, H. Tang, J. Zhang, X. Xia, J. Zhang, X. Lu, C. J. Brabec, F. Huang, *Adv. Mater.* **2022**, *34*, 2110587.
- [53] H. Kassem, A. Salehi, M. Kahrizi, *Energy Tech* **2024**, *12*, 2301032.
- [54] D. Liu, M. K. Gangishetty, T. L. Kelly, *J. Mater. Chem. A* **2014**, *2*, 19873.
- [55] D. Liu, J. Yang, T. L. Kelly, *J. Am. Chem. Soc.* **2014**, *136*, 17116.
- [56] S. Colodrero, *Mater. Sci.* **2017**, *4*, 956.
- [57] S. P. Koiry, P. Jha, C. Sridevi, D. Gupta, V. Putta, A. K. Chauhan, *Mater. Today Commun.* **2023**, *36*, 106418.
- [58] M. Zhang, M. Lyu, H. Yu, J. Yun, Q. Wang, L. Wang, *Chem. A Eur. J.* **2015**, *21*, 434.
- [59] H. Lu, Y. Ma, B. Gu, W. Tian, L. Li, *J. Mater. Chem. A* **2015**, *3*, 16445.

- [60] Y. Yang, Q. Xiong, J. Wu, Y. Tu, T. Sun, G. Li, X. Liu, X. Wang, Y. Du, C. Deng, L. Tan, Y. Wei, Y. Lin, Y. Huang, M. Huang, W. Sun, L. Fan, Y. Xie, J. Lin, Z. Lan, V. Stacchini, A. Musilenko, Q. Hu, P. Gao, A. Abate, M. K. Nazeeruddin, *Adv. Mater.* **2023**, *36*, 2310800.
- [61] W. Ren, J. Ren, Y. Wu, S. Li, Q. Sun, Y. Hao, *Adv. Funct. Mater.* **2024**, *34*, 2311260.
- [62] Z. Q. Lin, H. W. Qiao, Z. R. Zhou, Y. Hou, X. Li, H. G. Yang, S. Yang, *J. Mater. Chem. A* **2020**, *8*, 17670.
- [63] J. V. Patil, S. S. Mali, C. K. Hong, *ACS Appl. Mater. Interfaces* **2020**, *12*, 27176.
- [64] M. J. Jeong, S. W. Jeon, S. Y. Kim, J. H. Noh, *Adv. Energy Mater.* **2023**, *13*, 2300698.
- [65] T. Ye, K. Wang, Y. Hou, D. Yang, N. Smith, B. Magill, J. Yoon, R. R. H. H. Mudiyansele, G. A. Khodaparast, K. Wang, S. Priya, *J. Am. Chem. Soc.* **2021**, *143*, 4319.
- [66] M. Li, S. Liu, F. Qiu, Z. Zhang, D. Xue, J. Hu, *Adv. Energy Mater.* **2020**, *10*, 2000501.
- [67] W. Zhang, L. Wan, S. Fu, X. Li, J. Fang, *J. Mater. Chem. A* **2020**, *8*, 6546.
- [68] J. Song, H. Xie, E. L. Lim, Y. Li, T. Kong, Y. Zhang, X. Zhou, C. Duan, D. Bi, *Sol. RRL* **2022**, *6*, 2100880.
- [69] W.-M. Gu, K.-J. Jiang, F. Li, G.-H. Yu, Y. Xu, X.-H. Fan, C.-Y. Gao, L.-M. Yang, Y. Song, *Chem. Eng. J.* **2022**, *444*, 136644.
- [70] L. Qi, G. Du, G. Zhu, Y. Wang, L. Yang, J. Zhang, *ACS Appl. Mater. Interfaces* **2023**, *15*, 41109.
- [71] H. Choi, H. Lim, H. Kim, J. Lim, M. Park, C. S. Pathak, S. Song, *J. Mater. Chem. A* **2023**, *11*, 16363.
- [72] X. Zheng, J. Troughton, N. Gasparini, Y. Lin, M. Wei, Y. Hou, J. Liu, K. Song, Z. Chen, C. Yang, B. Turedi, A. Y. Alsalloum, J. Pan, J. Chen, A. A. Zhumekenov, T. D. Anthopoulos, Y. Han, D. Baran, O. F. Mohammed, E. H. Sargent, O. M. Bakr, *Joule* **2019**, *3*, 1963.
- [73] F. Cheng, R. He, S. Nie, C. Zhang, J. Yin, J. Li, N. Zheng, B. Wu, *J. Am. Chem. Soc.* **2021**, *143*, 5855.
- [74] E. H. Jung, N. J. Jeon, E. Y. Park, C. S. Moon, T. J. Shin, T.-Y. Yang, J. H. Noh, J. Seo, *Nature* **2019**, *567*, 511.
- [75] N. E. Jackson, K. L. Kohlstedt, B. M. Savoie, M. Olvera De La Cruz, G. C. Schatz, L. X. Chen, M. A. Ratner, *J. Am. Chem. Soc.* **2015**, *137*, 6254.
- [76] A. Khasbaatar, Z. Xu, J.-H. Lee, G. Campillo-Alvarado, C. Hwang, B. N. Onusaitis, Y. Diao, *Chem. Rev.* **2023**, *123*, 8395.
- [77] M. Brinkmann, *J. Polym. Sci. B Polym. Phys.* **2011**, *49*, 1218.
- [78] F. S. Kim, G. Ren, S. A. Jenekhe, *Chem. Mater.* **2011**, *23*, 682.
- [79] H. Sirringhaus, P. J. Brown, R. H. Friend, M. M. Nielsen, K. Bechgaard, B. M. W. Langeveld-Voss, A. J. H. Spiering, R. A. J. Janssen, E. W. Meijer, P. Herwig, D. M. De Leeuw, *Nature* **1999**, *401*, 685.
- [80] K. E. Aasmundtveit, E. J. Samuelsen, M. Guldstein, C. Steinsland, O. Flornes, C. Fagermo, T. M. Seeberg, L. A. A. Pettersson, O. Inganäs, R. Feidenhans'l, S. Ferrer, *Macromolecules* **2000**, *33*, 3120.
- [81] K. Sethuraman, S. Ochial, K. Kojima, T. Mizutani, *Appl. Phys. Lett.* **2008**, *92*, 183302.
- [82] D. M. DeLongchamp, B. M. Vogel, Y. Jung, M. C. Gurau, C. A. Richter, O. A. Kirillov, J. Obrzut, D. A. Fischer, S. Sambasivan, L. J. Richter, E. K. Lin, *Chem. Mater.* **2005**, *17*, 5610.
- [83] K. Yamamoto, S. Ochial, X. Wang, Y. Uchida, K. Kojima, A. Ohashi, T. Mizutani, *Thin Solid Films* **2008**, *516*, 2695.
- [84] G. Wang, N. Persson, P.-H. Chu, N. Kleinhenz, B. Fu, M. Chang, N. Deb, Y. Mao, H. Wang, M. A. Grover, E. Reichmanis, *ACS Nano* **2015**, *9*, 8220.
- [85] G. M. Newbloom, F. S. Kim, S. A. Jenekhe, D. C. Pozzo, *Macromolecules* **2011**, *44*, 3801.
- [86] A. R. Aiyar, J.-I. Hong, J. Izumi, D. Choi, N. Kleinhenz, E. Reichmanis, *ACS Appl. Mater. Interfaces* **2013**, *5*, 2368.
- [87] M. Chang, J. Lee, N. Kleinhenz, B. Fu, E. Reichmanis, *Adv. Funct. Mater.* **2014**, *24*, 4457.
- [88] M. S. Vezie, S. Few, I. Meager, G. Pieridou, B. Döring, R. S. Ashraf, A. R. Goñi, H. Bronstein, I. McCulloch, S. C. Hayes, M. Campoy-Quiles, J. Nelson, *Nat. Mater.* **2016**, *15*, 746.
- [89] N. Y. Nia, F. Matteocci, L. Cina, A. Di Carlo, *ChemSusChem* **2017**, *10*, 3854.
- [90] N. Yaghoobi Nia, M. Bonomo, M. Zendehele, E. Lamanna, M. M. H. Desoky, B. Paci, F. Zurlo, A. Generosi, C. Barolo, G. Viscardi, P. Quagliotto, A. Di Carlo, *ACS Sustain. Chem. Eng.* **2021**, *9*, 5061.
- [91] M. Park, J.-S. Park, I. K. Han, J. Y. Oh, *J. Mater. Chem. A* **2016**, *4*, 11307.
- [92] N. Yaghoobi Nia, E. Lamanna, M. Zendehele, A. L. Palma, F. Zurlo, L. A. Castriotta, A. Di Carlo, *Small* **2019**, *15*, 1904399.
- [93] J. W. Jung, J.-S. Park, I. K. Han, Y. Lee, C. Park, W. Kwon, M. Park, *J. Mater. Chem. A* **2017**, *5*, 12158.
- [94] H.-C. V. Tran, W. Jiang, M. Lyu, H. Chae, *J. Phys. Chem. C* **2020**, *124*, 14099.
- [95] S. N. Habisreutinger, T. Leijtens, G. E. Eperon, S. D. Stranks, R. J. Nicholas, H. J. Snaith, *Nano Lett.* **2014**, *14*, 5561.
- [96] J. Xiao, J. Shi, H. Liu, Y. Xu, S. Lv, Y. Luo, D. Li, Q. Meng, Y. Li, *Adv. Energy Mater.* **2015**, *5*, 1401943.
- [97] J. Ye, X. Li, J. Zhao, X. Mei, Q. Li, *RSC Adv.* **2016**, *6*, 36356.
- [98] M. Li, J. Shao, Y. Jiang, F. Qiu, S. Wang, J. Zhang, G. Han, J. Tang, F. Wang, Z. Wei, Y. Yi, Y. Zhong, J. Hu, *Angew. Chem. Int. Ed.* **2021**, *60*, 16388.
- [99] D. Xu, Z. Gong, Y. Jiang, Y. Feng, Z. Wang, X. Gao, X. Lu, G. Zhou, J.-M. Liu, J. Gao, *Nat. Commun.* **2022**, *13*, 7020.
- [100] F. Cao, F. Cheng, X. Huang, X. Dai, Z. Tang, S. Nie, J. Yin, J. Li, N. Zheng, B. Wu, *Adv. Funct. Mater.* **2022**, *32*, 2201423.
- [101] J. Wang, Q. Hu, M. Li, H. Shan, Y. Feng, Z.-X. Xu, *Sol. RRL* **2020**, *4*, 2000109.
- [102] Y. Liu, B. He, J. Duan, Y. Zhao, Y. Ding, M. Tang, H. Chen, Q. Tang, *J. Mater. Chem. A* **2019**, *7*, 12635.
- [103] J. Peng, D. Walter, Y. Ren, M. Tebyetekerwa, Y. Wu, T. Duong, Q. Lin, J. Li, T. Lu, M. A. Mahmud, O. L. C. Lem, S. Zhao, W. Liu, Y. Liu, H. Shen, L. Li, F. Kremer, H. T. Nguyen, D.-Y. Choi, K. J. Weber, K. R. Catchpole, T. P. White, *Science* **2021**, *371*, 390.
- [104] A. Marrocchi, D. Lanari, A. Facchetti, L. Vaccaro, *Energy Environ. Sci.* **2012**, *5*, 8457.
- [105] C.-M. Chen, T.-H. Jen, S.-A. Chen, *ACS Appl. Mater. Interfaces* **2015**, *7*, 20548.
- [106] J. B. Howard, S. Noh, A. E. Beier, B. C. Thompson, *ACS Macro Lett.* **2015**, *4*, 725.
- [107] G. Zhang, Y. Ohta, T. Yokozawa, *Macromol. Rapid Commun.* **2018**, *39*, 1700586.
- [108] B. Koo, E. M. Sletten, T. M. Swager, *Macromolecules* **2015**, *48*, 229.
- [109] F. Di Giacomo, A. Fakharuddin, R. Jose, T. M. Brown, *Energy Environ. Sci.* **2016**, *9*, 3007.
- [110] Z. Liu, P. You, C. Xie, G. Tang, F. Yan, *Nano Energy* **2016**, *28*, 151.
- [111] Y. Y. Kim, T.-Y. Yang, R. Suhonen, A. Kemppainen, K. Hwang, N. J. Jeon, J. Seo, *Nat. Commun.* **2020**, *11*, 5146.
- [112] F. Matteocci, L. Cina, F. Di Giacomo, S. Razza, A. L. Palma, A. Guidobaldi, A. D'Epifanio, S. Licocchia, T. M. Brown, A. Reale, A. Di Carlo, *Prog. Photovolt.* **2016**, *24*, 436.
- [113] S. Razza, F. Di Giacomo, F. Matteocci, L. Cina, A. L. Palma, S. Casaluci, P. Cameron, A. D'Epifanio, S. Licocchia, A. Reale, T. M. Brown, A. Di Carlo, *J. Power Sources* **2015**, *277*, 286.
- [114] Y. Ren, K. Zhang, Z. Lin, X. Wei, M. Xu, X. Huang, H. Chen, S. Yang, *Nano-Micro Lett.* **2023**, *15*, 182.
- [115] L. Qiu, S. He, L. K. Ono, S. Liu, Y. Qi, *ACS Energy Lett.* **2019**, *4*, 2147.
- [116] R. D. McCullough, *Adv. Mater.* **1998**, *10*, 93.

- [117] J. H. Bannock, S. H. Krishnadasan, A. M. Nightingale, C. P. Yau, K. Khaw, D. Burkitt, J. J. M. Halls, M. Heeney, J. C. De Mello, *Adv. Funct. Mater.* **2013**, 23, 2123.
- [118] R. Po, A. Bernardi, A. Calabrese, C. Carbonera, G. Corso, A. Pellegrino, *Energy Environ. Sci.* **2014**, 7, 925.
- [119] M. Osaka, H. Benten, L.-T. Lee, H. Ohkita, S. Ito, *Polymer* **2013**, 54, 3443.
- [120] X. Yu, D. Gao, Z. Li, X. Sun, B. Li, Z. Zhu, Z. Li, *Angew. Chem. Int. Ed.* **2023**, 62, 202218752.
- [121] Q. Liao, Y. Wang, M. Hao, B. Li, K. Yang, X. Ji, Z. Wang, K. Wang, W. Chi, X. Guo, W. Huang, *ACS Appl. Mater. Interfaces* **2022**, 14, 43547.
- [122] M. Ahn, M.-J. Kim, K.-R. Wee, *J. Org. Chem.* **2019**, 84, 12050.
- [123] C. Lim, Y. Kim, S. Lee, H. H. Park, N. J. Jeon, B. J. Kim, *J. Mater. Chem. A* **2023**, 11, 6615.
- [124] Z. Chen, Z. Hu, Z. Wu, X. Liu, Y. Jin, M. Xiao, F. Huang, Y. Cao, *J. Mater. Chem. A* **2017**, 5, 19447.
- [125] A. Islam, J. Li, M. Pervaiz, Z. Lu, M. Sain, L. Chen, X. Ouyang, *Adv. Energy Mater.* **2019**, 9, 1803354.
- [126] S. Wang, A. Wang, X. Deng, L. Xie, A. Xiao, C. Li, Y. Xiang, T. Li, L. Ding, F. Hao, *J. Mater. Chem. A* **2020**, 8, 12201.
- [127] A. F. Latypova, N. A. Emelianov, D. O. Balakirev, P. K. Sukhorukova, N. K. Kalinichenko, P. M. Kuznetsov, Y. N. Luponosov, S. M. Aldoshin, S. A. Ponomarenko, P. A. Troshin, L. A. Frolova, *ACS Appl. Energy Mater.* **2022**, 5, 5395.
- [128] A. Abudulimu, R. Sandoval-Torrientes, I. Zimmermann, J. Santos, M. K. Nazeeruddin, N. Martín, *J. Mater. Chem. A* **2020**, 8, 1386.
- [129] X. Yu, Z. Li, X. Sun, C. Zhong, Z. Zhu, Z. Li, A. K.-Y. Jen, *Nano Energy* **2021**, 82, 105701.
- [130] M. Ulfa, T. Zhu, F. Goubard, T. Pauporté, *J. Mater. Chem. A* **2018**, 6, 13350.
- [131] Q. Wang, Y. Qin, M. Li, L. Ye, Y. Geng, *Adv. Energy Mater.* **2020**, 10, 2002572.
- [132] M. An, Q. Bai, S. Y. Jeong, J. Ding, C. Zhao, B. Liu, Q. Liang, Y. Wang, G. Zhang, H. Y. Woo, X. Qiu, L. Niu, X. Guo, H. Sun, *Adv. Energy Mater.* **2023**, 13, 2301110.
- [133] P. Gao, A. R. Bin Mohd Yusoff, M. K. Nazeeruddin, *Nat. Commun.* **2018**, 9, 5028.
- [134] A. H. Proppe, M. Wei, B. Chen, R. Quintero-Bermudez, S. O. Kelley, E. H. Sargent, *J. Am. Chem. Soc.* **2019**, 141, 14180.
- [135] N. E. Persson, P.-H. Chu, M. McBride, M. Grover, E. Reichmanis, *Acc. Chem. Res.* **2017**, 50, 932.
- [136] S. K. K. Aung, A. Vijayan, T. Seetawan, G. Boschloo, *Sol. RRL* **2022**, 6, 2100773.
- [137] C. Teixeira, P. Spinelli, L. A. Castriotta, D. Müller, S. Öz, L. Andrade, A. Mendes, A. D. Carlo, U. Würfel, K. Wojciechowski, D. Forgács, *Adv. Funct. Mater.* **2022**, 32, 2206761.
- [138] F. Cheng, S. Zhan, Y. Cai, F. Cao, X. Dai, R. Xu, J. Yin, J. Li, N. Zheng, B. Wu, *J. Am. Chem. Soc.* **2023**, 145, 20081.
- [139] A. Wijesekara, M. Walker, Y. Han, D. Walker, S. Huband, R. A. Hatton, *Adv. Energy Mater.* **2021**, 11, 2102766.
- [140] A. M. K. Fehr, T. G. Deutsch, F. M. Toma, M. S. Wong, A. D. Mohite, *ACS Energy Lett.* **2023**, 8, 4976.
- [141] Q. Fu, H. Liu, S. Li, T. Zhou, M. Chen, Y. Yang, J. Wang, R. Wang, Y. Chen, Y. Liu, *Angew. Chem. Int. Ed.* **2022**, 61, 202210356.
- [142] Y. Hu, T. Niu, Y. Liu, Y. Zhou, Y. Xia, C. Ran, Z. Wu, L. Song, P. Müller-Buschbaum, Y. Chen, W. Huang, *ACS Energy Lett.* **2021**, 6, 2917.



Xiaozhen Huang received his B.Sc. (2022) degree from Guizhou Minzu University. He is recently pursuing his M.Sc. under the supervision of Prof. Yang Wang at Strait Institute of Flexible Electronics (SIFE, Future technologies) in Fujian Normal University. His research interests mainly focus on organic functional materials and their applications in solution-processable photovoltaic devices.



Mingwei An received his Ph.D. degree from Xiamen University of China (2021) under the supervision of Prof. Suyuan Xie. Then he worked as a postdoctoral fellow in Prof. Xugang Guo's group at Southern University of Science and Technology. In 2023, he joined the Strait Institute of Flexible Electronics (SIFE, Future technologies) in Fujian Normal University as an associate Professor. His research interests focus on design and synthesis of innovative organic semiconductor materials for optoelectronic devices.



Yang Wang received his B.Sc. degree from University of Science and Technology of China (2009) and Ph.D. degree in Changchun Institute of Applied Chemistry, Chinese Academy of Sciences (CAS) under the supervision of Prof. Lixiang Wang (2015). Then, he worked as a postdoctoral fellow at Tsing Hua University (Chinese Taiwan), Southern University of Science and Technology and Xiamen University successively. In 2022, he obtained Professor position in Fujian Normal University to continue his research interest including novel organic semiconductor materials and their applications in optoelectronic devices.